Mitochondrial diabetes in mice expressing a dominant-negative allele of nuclear respiratory factor-1 (NRF-1) in pancreatic β-cells

Fionnuala Morrish[1], Ian R. Sweet[2], David M. Hockenbery[1*]

[1]Division of Clinical Research, Fred Hutchinson Cancer Center, Seattle, WA.

[2]University of Washington Diabetes Institute, University of Washington, Seattle, WA

Correspondence: dhockenb@fredhutch.org

Keywords: diabetes, mitochondria, c-Myc

Abbreviations: DNNRF-1, dominant-negative nuclear respiratory factor-1, GSIS, glucose-stimulated insulin secretion, NRF-1, nuclear respiratory factor-1, OCR, oxygen consumption rate, PCR, polymerase chain reaction, T1D, type 1 diabetes

SUMMARY

Genetic polymorphisms in nuclear respiratory factor-1 (NRF-1), a key transcriptional regulator of nuclear-encoded mitochondrial proteins, have been linked to diabetes. Homozygous deletion of NRF-1 is embryonic lethal. Our goal was to generate mice with β-cell-specific reduction in NRF-1 function to investigate the relationship between NRF-1 and diabetes. We report the generation of mice expressing a dominant-negative allele of NRF-1 (DNNRF-1) in pancreatic β-cells. Heterozygous transgenic mice had high fed blood glucose levels detected at 3 wks of age, which persisted through adulthood. Plasma insulin levels in DNNRF-1 transgenic mice were reduced, while insulin sensitivity remained intact in young animals. Islet size was reduced with increased numbers of apoptotic cells, and insulin content in islets by immunohistochemistry was low. Glucose-stimulated insulin secretion in isolated islets was reduced in DNNRF-1-mice, but partially rescued by KCl, suggesting that decreased mitochondrial function contributed to the insulin secretory defect. Electron micrographs demonstrated abnormal mitochondrial morphology in β-cells. Expression of NRF-1 target genes Tfam, Tfb1m and Tfb2m, and islet cytochrome c oxidase and succinate dehydrogenase activities were reduced in DNNRF-1-mice. Rescue of mitochondrial function with low level activation of transgenic c-Myc in β-cells was sufficient to restore β-cell mass and prevent diabetes. This study demonstrates that reduced NRF-1 function can lead to loss of β-cell function and establishes a model to study the interplay between regulators of bi-genomic gene transcription in diabetes.

INTRODUCTION

In the pancreatic β-cell, mitochondrial function is required for the coupling of glucose metabolism to insulin secretion (Maechler et al., 2006; Jensen et al., 2008; Matschinsky and Collins, 1997; Wiederkehr and Wollheim, 2012). Extensive evidence shows that reduction of mitochondrial activity in islets and insulin-secreting cell lines by a variety of insults, including inhibition of cytoplasmic NADH shuttles or cataplerotic/anaplerotic functions, and lipotoxicity, inhibits glucose-stimulated insulin secretion (GSIS) (Maedler et al., 2001; Antinozzi et al., 2002; Rubi et al., 2004; Noda et al., 2002; Campbell and Newgard, 2021). The effects of mitochondrial dysfunction reflect the role of mitochondria in β−cell ATP generation, as increased energy charge (ATP/ADP) is a key factor in closing KATP channels that leads to elevated flux of calcium through L-type calcium channels and stimulation of trafficking and exocytosis of insulin granules. Decreased ATP production therefore will result in diminished insulin secretion.

Pancreatic β-cell dysfunction is observed with mutations in mitochondrial DNA in some diabetes patients (Kobayashi et al, 1997; Katagiri et al., 1994; Bensch et al., 2009; Karaa and Goldstein, 2015). Transcriptional regulators of mitochondrial biogenesis include peroxisome proliferator-activated receptor gamma coactivator 1 alpha, beta and PGC-1-related coactivator (PGC-1α, PGC-1β, PRC), nuclear respiratory factors 1 and 2 (NRF-1, NRF-2), and estrogen-related receptor alpha (ERRα) (Handschin and Spiegelman, 2006; Scarpulla, 2008). Alterations in the expression of these transcription factors may also occur in diabetic islets. For example, PGC-1α expression is reduced in islets from Type 2 diabetes (T2D) patients (Ling et al., 2008).

An important downstream target of these mitochondrial regulators is the transcription factor *TFAM*, a nuclear-encoded gene that regulates the transcription and replication of mitochondrial DNA (Kang et al., 2007). Targeted knockout of *Tfam* in β-cells results in impaired insulin secretion and β cell loss (Silva et al., 2000). Diabetes in this model was transient as mice older than 20 wks showed normalization of fasting blood glucose due to incomplete knockout in β-cells.

Many of the effects of PGC-1 and related co-activators are mediated through activation of the transcription factor NRF-1 (Scarpulla, 2008). NRF-1 regulates genes required for

mitochondrial biogenesis, including *TFAM*, *TFB1M* and *TFB2M* transcription factors, and subunits of the respiratory complexes of the electron transport chain, including all 10 nuclear-encoded genes for cytochrome c oxidase (Gleyzer et al., 2005; Dhar et al., 2009). There are several reports linking genetic polymorphisms in *NRF-1* with type 2 diabetes (Cho et al., 2005; Gaulton et al., 2008; Liu et al., 2008). However, the role of NRF-1 in β-cell function is unknown, as *Nrf-1* knockout is embryonic lethal between day E3.5 and E6.5 with decreased cell proliferation and mtDNA content (Huo and Scarpulla, 2001). To address the role of Nrf-1 in regulating mitochondrial function in pancreatic β-cells, we have generated transgenic mice that selectively express a dominant-negative allele of *Nrf-1* (*Dnnrf-1*) in pancreatic β-cells under the control of the rat *Ins2* promoter. InsDNNRF-1ER^{TAM} transgenic mice develop diabetes at an early age that persists over the lifetime of the mouse and is associated with weight loss, decreased serum insulin and β-cell loss due to apoptosis. This model provides further genetic evidence of a critical role for mitochondria in normal glucose-stimulated insulin secretion and suggests a role for NRF-1 as a key regulator of mitochondrial biogenesis in β-cells.

RESULTS

Generation of transgenic mice expressing dominant-negative Nrf-1

Using a previously published human dominant-negative NRF-1 construct with a deleted transactivation domain (DNNRF-1), we generated the plasmid pIns-*DNNRF-1ER^{TAM}* containing an in-frame fusion to the estrogen receptor under control of the rat *Ins2* promoter (Figure 1A) (Morrish et al., 2003; Wu et al., 1999; Gonen and Assaraf, 2010; Tokusumi et al., 2004; Kherrouche et al., 2004). Founder mice were screened by PCR amplification of a region spanning the 3' end of *Dnnrf-1* and the 5' end of the fused estrogen receptor. A total of 3 positive founders were generated and two successfully established founder lines (#2 and #3). Southern analysis was used to demonstrate transgene integration and copy number (Figure 1B). Copy numbers were estimated to be 10 and 1-2 by Southern blot for founders #2 and #3, respectively

(data shown for founder #2 in Figure 1B). The transgene was transmitted to 50% of progeny. Heterozygous pups were normal in size compared to their wild-type littermates.

Ins-DNNRF-1ER^{TAM} transgenic mice are diabetic

Fasting hyperglycemia (459.2+/-40.0 mg/dl; 497.4+/-29.8 mg/dl) and glucosuria (data not shown) were observed in both founder lines of transgenic Ins-*DNNRF-1ER^{TAM}* mice at 6-8 wks of age without tamoxifen treatment (Figure 1C). Analysis of fed glucose levels over time detected hyperglycemia as early as 3 wks of age (Supplemental Figure 1). This suggested that leaky activation of the DNNRF-1ER^{TAM} protein was sufficient to induce diabetes and all further studies were conducted in the founder line #2 in the absence of tamoxifen. Fasting blood glucose data are shown for males in Figure 1C; females also had a diabetic phenotype (mean 428+/-32) with a slightly lower mean fasting glucose. Fasting serum insulin concentrations were significantly less than control levels in 8 wk old transgenic mice (control 0.57+/- 0.108 ng/ml, DNNRF-1 0.257 +/- 0.122 ng/ml, p=0.013) (Figure 1D). Significant reductions were also observed in serum C-peptide concentrations (control 1060 +/- 112 pM, DNNRF-1 709 +/- 132 pM, p=0.012) (Figure 1E). Treatment with insulin demonstrated normal insulin sensitivity at 2 months of age (Figure 1F), but insulin resistance was present at 9 months (data not shown). At 26 wk of age, transgenic mice showed persistently elevated fasting blood glucose (control 163+/- 9.8 mg/dL, DNNRF-1 > 600 mg/dL) and a significant reduction in body weight (control 41+/- 1.5 gm, DNNRF-1, 29+/- 1.7 gm, p=0.013) (Figure 1G, H).

Pancreatic β-cell depletion in Ins-*DNNRF-1ER^{TAM}* mice

We analyzed histological sections from pancreata of Ins-*DNNRF-1ER^{TAM}* mice presenting with hyperglycemia at two months of age. H&E-stained sections showed small, deformed islets (Figure 2A, B). To determine if the alterations in islet morphology in Ins-*DNNRF-1ER^{TAM}* mice were associated with increased apoptotic cell death, we immunostained paraffin-fixed pancreatic sections for cleaved caspase-3. Numerous caspase-3-positive cells were present within islets from Ins-*DNNRF-1ER^{TAM}* mice, while caspase-3 staining in wild-type littermates was

confined to a few peripheral islet cells (Figure 2C, D), as previously reported (Ladiges et al., 2005).

Staining of paraffin sections with an anti-insulin antibody showed sparse, scattered staining in Ins-*DNNRF-1ER*^{TAM} mice at two months of age (Figure 2E, F) compared to islets in wild-type littermates. The loss of insulin staining persisted in mice at 6 mos of age (Figure 2G, H).

Quantitation of islet morphology demonstrated that average islet area was decreased (Supplemental Figure 2A) and individual islet cells were crowded, with increased nuclei per unit islet area (Supplemental Figure 2B). These pathological changes were limited to the islets, with no histological changes in pancreatic acini. Quantitative differences in apoptotic cells and insulin staining between wild-type and transgenic islets were statistically significant (Supplemental Figure 2C, D).

Staining with anti-glucagon antibody demonstrated a predominance of α-cells in islets from DNNRF-1 transgenic mice (Supplemental Figure 3).

DNNRF-1 and target genes

We performed qRT-PCR to determine if DNNRF-1ER^{TAM} altered the expression of *Tfam*, *Tfb1m*, and *Tfb2m*, NRF-1 target genes involved in regulation of mitochondrial transcription. Expression of the three genes was significantly lower in DNNRF-1 transgenics (>80% reduction; Supplemental Table 1). The *Ins2* promoter used in this study has been shown to result in transgene expression in the hypothalamus and at low levels, in kidney and duodenum, in addition to pancreatic β−cells (Wicksteed et al., 2010). Hypothalamic expression of *Tfam*, *Tfb1m* and *Tfb2m* was not significantly different between wild type and DNNRF-1-mice (Supplemental Table 1). A non-mitochondrial target of NRF-1 transactivation normally expressed in pancreatic β-cells, *Vsnl1*, was reduced in expression in DNNRF-1 islets by immunohistochemistry (Supplemental Figure 4) (Fu et al., 2009; Dai et al., 2006).

Mitochondrial function and morphology in pIns-DNNRF-1ER^{TAM} islets

To determine if the reduced insulin staining and altered morphology of Ins-*DNNRF-1ER^{TAM}* islets were linked to diminished NRF-1-dependent respiratory chain function, we examined cytochrome c oxidase (COX) and succinate dehydrogenase (SDH) activities in sections using histochemical assays. NRF-1 regulates the transcription of all 10 COX nuclear genes, and all 4 SDH subunits, as well as the mitochondrial transcription factor TFAM (Gleyzer et al., 2005; Dhar et al., 2008; Piantadosi and Suliman, 2008; Au and Scheffler, 1998). We observed a reduction in COX and SDH activities in islets of Ins-DNNRF-1ER^{TAM} mice at two months of age (Figure 3A-D).

In electron micrographs of isolated islets, cells were identified that exhibited the characteristic appearance of insulin secretory granules, with a central dense core and a surrounding halo (Figure 3E, F). In Ins-*DNNRF-1ER^{TAM}* mice, β-cells contained numerous elongated mitochondria with diffusely electron-dense matrix material obscuring the cristae (Figure 3F and insert). This appearance suggests accumulation of insoluble protein, possibly linked to incomplete assembly of ETC protein complexes (Morrish et al., 2003; Margineantu et al., 2007). β-cells in islets from both wild type and Ins-*DNNRF-1ER^{TAM}* mice were similar in size (Supplemental Figure 5A). A trend towards increased mitochondrial number and area in Ins-*DNNRF-1ER^{TAM}* mice did not reach statistical significance (Supplemental Figure 5B, C). However, we did find a significant increase in the number of secretory granules per cell, possibly consistent with a secretory defect (Supplemental Figure 5D).

Perfusion analysis of oxygen consumption rate (OCR) and glucose-stimulated insulin secretion (GSIS) was performed on isolated islets. DNNRF-1 islets had significantly lower OCR in the presence of 3 mM glucose and this difference further increased with the addition of 20 mM glucose (Figure 4A). The GSIS was also significantly reduced, to less than 0.04 ng/min/100 transgenic islets, and there was no significant response to higher glucose concentrations (Figure 4B).

Static islet insulin assays confirmed a reduction in GSIS in DNNRF-1 transgenics (Supplemental Figure 6). Insulin secretion was partially rescued in response to added KCl in DNNRF-1 islets. These results are consistent with defective mitochondrial metabolism as a

contributing mechanism of β-cell dysfunction in Ins-*DNNRF-1ER*^{TAM} mice. ATP levels (normalized to total protein) in isolated islets from Ins-*DNNRF-1ER*^{TAM} mice were less than 50% of control levels (Supplemental Figure 7).

Myc transgene eliminates diabetes in Ins-*DNNRF-1-ER*^{TAM} mice

In previous work we showed that the MYC oncoprotein and NRF-1 shared gene targets, due to common binding sites in promoters of a subset of nuclear-encoded mitochondrial genes (Morrish et al., 2003). Subsequent studies have confirmed MYC's role in regulation of bi-genomic transcription and demonstrate that MYC, like NRF-1, is involved in regulation of mitochondrial biogenesis (Li et al., 2005; Popay et al., 2021). MYC expression can trigger mitochondrial pathways of apoptosis under some conditions. Dual expression of MYC and DNNRF-1 suppressed MYC-induced apoptosis in fibroblasts under nutrient-deprived conditions and improved mitochondrial function, suggesting that restoration of balanced mitochondrial gene expression and mitochondrial function opposes apoptosis (Morrish et al., 2003). To determine if MYC would likewise suppress DNNRF-1-induced cytotoxicity in pancreatic β-cells, we generated Ins-*DNNRF-1ER*^{TAM} / Ins-*MycER*^{TAM} mice.

We found that the double transgenic mice had normal levels of fasting blood glucose, and normal responses to glucose challenge (Figure 5A, B). This result was observed without tamoxifen treatment, which is normally required for nuclear translocation of the MYC-ER^{TAM} protein, suggesting leaky activation of MYC-ER^{TAM} protein in β-cells. The distribution of insulin staining in pancreatic islets was similar to controls (Supplemental Figure 8), confirmed as shown by quantitative image analysis (control insulin staining 92.6 +/- 1.0 %, Ins-*DNNRF-1ER*^{TAM} / Ins-*MycER*^{TAM} 93.7 +/- 0.7%). Inducible activation of c-MYC in adult β cells produces rapid islet involution due to apoptosis, with almost complete ablation of β cells within 6-10 days (Pelengaris et al., 2002). Others have shown that, in the absence of tamoxifen, Ins-*MycER*^{TAM} transgenic mice exhibit changes in β-cell proliferation and glucose-stimulated insulin secretion consistent with MYC-ER^{TAM} activity (Pascal et al., 2008). This activity appears to be sufficient to rescue the negative effects of DNNRF-1 on glucose homeostasis and islet morphology.

DISCUSSION

In this study, we show that expression of a dominant-negative mutant of nuclear respiratory factor 1 (DNNRF-1) in pancreatic β-cells results in the early onset of diabetes. Our data show that baseline serum insulin levels for Ins-*DNNRF-1ER*^{TAM} transgenic mice were 2-3 fold less than controls despite high levels of blood glucose. Blood glucose in Ins-*DNNRF-1ER*^{TAM} mice normalized with 1 mU/g insulin i.p., confirming that DNNRF-1 expression in β cells produced insulin deficiency rather than systemic insulin resistance. The loss of insulin sensitivity found in older animals is likely a consequence of sustained hyperglycemia as observed in mouse models of type 1 diabetes and patients with T1D (Unger and Grundy, 1985; Perseghin et al., 2003; Hong et al., 2007). Although the *Ins2* promoter is known to produce expression of transgenes in hypothalamus, kidney and duodenum, reduced expression of NRF-1 targets *Tfam*, *Tfb1m* and *Tfb2m* in hypothalami from DNNRF-1-mice was not evident, and we could not demonstrate expression of *Dnnrf-1* in kidney or duodenum.

Apoptotic cells were evident in transgenic islets by light and electron microscopy and immunostaining for cleaved caspase-3 confirmed an increased apoptotic rate. This differs from mice with β-cell-selective knockout of *Tfam*, a NRF-1 target, which had reduced β-cell mass without evidence of apoptosis and points to a more severe phenotype when multiple NRF-1 targets are inactivated (Silva et al., 2000).

In addition to apoptotic loss of β-cells, it is probable that DNNRF-1 decreases glucose-stimulated insulin secretion via reduced expression of mitochondrial respiratory chain proteins regulated by NRF-1 (Scarpulla, 2008). Mitochondrial dysfunction in surviving β-cells is indicated by the absence of detectable respiratory activity, low cytochrome oxidase and succinate dehydrogenase activity by histochemistry, and abnormal mitochondrial ultrastructure, without a decrease in mitochondrial content. Reduction of cytochrome oxidase and succinate dehydrogenase activities by DNNRF-1 is consistent with the regulation of complex II and IV subunits by NRF-1 (Dhar et al., 2008; Piantadosi and Suliman, 2008; Au and Scheffler, 1998).

Mitochondrial diabetes is associated with mtDNA mutations and is estimated to account for less than 5 percent of patients with diabetes. Despite a high penetrance of this maternally inherited form of the disease, the average age of onset is 35-40 y, raising questions about the mechanism for gradual loss of islet cell function (Maassen et al., 2004). The majority of mtDNA mutations that result in diabetes are associated with alterations in mitochondrial protein synthesis. Diabetes occurs in association with a mtDNA mutation in the tRNA-Leu gene in patients with maternally inherited diabetes and deafness (MIDD), representing 0.5-3.0% of the diabetes population. The same mutation, MTLL1*MELAS3243G, when present at higher levels of heteroplasmy (>85%) is associated with MELAS (mitochondrial encephalopathy, lactic acidosis and stroke-like episodes), which may include diabetes in its presentation (Stark and Roden, 2007). Mitochondrial myopathies associated with diabetes include mutations affecting protein synthesis at tRNA-Lys in myoclonic epilepsy and ragged red fibers (MERRF), and Kearns-Sayre syndrome and chronic progressive external ophthalmoplegia (CPEO), both deletions involving tRNAs (Austin et al., 1998). Additionally, decreased insulin secretion has been described in MIDD, Kearns-Sayre and CPEO (Piccolo et al., 1989; Becker et al., 2002; Salles et al., 2007). Surprisingly, other mtDNA mutations, rearrangements or deletions associated with inherited diseases (Leber's hereditary optic neuropathy – ND4/6 mutation, Leigh's syndrome/NARP (Neuropathy, Ataxia and Retinitis Pigmentosa) – ATP6 mutation) are not associated with diabetes (Maassen et al., 2004).

The selective association of mitochondrial translation mutations with diabetes suggests that NRF-1 targets involved in mitochondrial translation such as *MRPS12* or mtDNA replication/ transcription (*TFAM*, *TFB1M*, *TFB2M*) may be critical for the mitochondrial diabetic phenotype (Gleyzer et al., 2005; Cam et al., 2004; Yau et al., 2021). Indeed, a common variant in *TFB1M* is associated with reduced insulin secretion, elevated postprandial glucose levels, and future risk of type 2 diabetes and analysis of *Tfb1m*$^{+/-}$ mice demonstrate a reduction in mitochondrially encoded proteins (Koeck et al., 2011). In these mice, GSIS is reduced by 36%, fuel-stimulated ATP by 25% and glucose stimulated oxygen consumption by 18%. Our findings for Ins-*DNNRF-1ER*^{TAM} transgenic mice are indicative of a more severe phenotype since there is a 70% reduction in

GSIS, a 60% reduction in ATP and glucose stimulated oxygen consumption was negligible. These differences are likely attributable to NRF-1's dual regulation of both mitochondrial-encoded and nuclear-encoded mitochondrial proteins and associated effects to disrupt electron transport chain protein assembly. Electron micrographs of β cells confirm that β-cells contained morphologically abnormal mitochondria filled with electron-dense matrix material obscuring the cristae. This appearance is reminiscent of mitochondria from serum-deprived cells expressing activated MYC that are also undergoing apoptosis and may represent misassembled proteins in the matrix prone to precipitation (Morrish et al., 2003; Margineantu et al., 2007).

We found that introduction of MycER^{TAM} targeted to β-cells, by generating double transgenic pIns-*DNNRF-1ER^{TAM}*/ pIns-*MycER^{TAM}* mice, suppressed the diabetic phenotype of pIns-DNNRF-1ER^{TAM} mice. This suggests that two pro-apoptotic factors with opposite effects on mitochondrial gene expression are capable of in vivo complementation or synergistic viability, as observed for NIH3T3 fibroblasts in vitro (Morrish et al., 2003). Direct transcription targets of Myc including mitochondrial genes overlapping with NRF-1 targets, recently shown to require specific interactions of Myc with host cell factor (HCF)-1 (Morrish et al., 2008; Popay et al., 2021). The NRF-1 binding motif is a non-canonical E-box that Myc binds in vitro and in vivo. The most likely explanation is a balancing of their effects on mitochondrial biogenesis, with restoration of mitochondrial oxidative phosphorylation and "unpriming" of mitochondrial pathways of apoptosis. The rescue of the diabetic phenotype is especially notable since both single transgenics are associated with insulin-deficient diabetes (*Dnnrf-1* this study; *Myc* (Piantadosi and Suliman, 2008)). Recent in vitro studies have demonstrated that there is sufficient Ins-*MycER^{TAM}* activity in the absence of tamoxifen to inhibit glucose-stimulated Ca^{2+} flux, mitochondrial hyperpolarization and insulin secretion in vitro (Pascal et al., 2008).

Although genetic polymorphisms in *NRF-1* have been linked to diabetes, this study is the first study to demonstrate a direct role for NRF-1 in β cell function and survival (Cho et al., 2005; Gaulton et al., 2008; Liu et al., 2008; Cam et al., 2004). This model provides a tool for future investigations into mitochondrial diabetes and opportunities to study the ameliorating effects of other regulatory factors involved in bi-genomic regulation of mitochondrial biogenesis.

Limitations of the study

The linkage of genetic polymorphisms in NRF-1 with type 2 diabetes in Korean, Han Chinese and Finnish populations has been suggested as an example of mitochondrial diabetes. Mitochondrial dysfunction can impair glucose tolerance via two mechanisms: decreased insulin production (effects on pancreatic β-cells) or insulin resistance (effects on peripheral tissues). Mitochondrial diabetes often involves both mechanisms (Lindroos et al., 2009). Our transgenic study is limited to effects on pancreatic β-cells, and in addition to potential differences in the degree of NRF-1 functional deficits between the mouse model and germline polymorphisms, is not designed to replicate the genetic association in human disease.

Analysis of pancreatic islet composition and glucose-stimulated insulin secretion support a role for DNNRF-1-dependent mitochondrial dysfunction in reduced insulin secretion in viable β-cells and in progressive loss of β-cells via apoptosis. The relative contribution of these mechanisms may depend on the extent of mitochondrial dysfunction, and our study did not attempt to explore additional mouse models with more limited NRF-1 impairment. Limited studies of islets obtained at autopsy in mitochondrial diabetes have also demonstrated β-cell depletion (Kobayashi et al., 1997).

We proposed one mechanism of mitochondrial dysfunction to be misassembly of mitochondrial electron transport chain complexes. While the appearance of diffusely electron-dense material in the mitochondrial matrix has been associated with reduced detergent extractability (Margineantu et al., 2007), we did not specifically test for the presence of incomplete ETC complexes in β-cells from DNNRF-1-mice.

METHODS

Plasmid construction

A truncated NRF-1 with the transcriptional activation site removed and fused to the hormone-binding domain of a modified estrogen receptor, DNNRF-1ER^{TAM}, has been described previously (Morrish et al., 2003; Wu et al., 1999; Gonen and Assaraf, 2010; Tokusumi et al., 2004;

Kherrouche et al., 2004). The rat insulin promoter expression plasmid was a gift from G. Evan (UCSF) and comprises 0.7 kb of the rat insulin promoter and 1.6 kb of the β-globin polyadenylation sequence in a pUC18 backbone (pIns) (Ohashi et al., 1991). DNNRF-1ER^{TAM} DNA was excised from pBabe vector by partial BamH1/BstI digest and blunt-ended with T4 DNA polymerase. The pIns plasmid was cut with BamHI and blunt-ended with T4 polymerase, and ligated to the DNNRF-1ER^{TAM} sequence. Since no unique restriction sites were present in the pUC18 vector, the insert was excised with SmaI and HindIII to generate two fragments (SmaI-SmaI and SmaI-HindIII) that were subsequently sub-cloned into the SmaI-HindIII site of pBluescript in a 3-way ligation. The final transgene construct was then excised from pBluescript as a 4.25 kb NotI-HindIII fragment. Purified DNA was resuspended for pronuclear injection in sterile buffer (10 mM Tris, 0.1 mM EDTA pH 7.4) at a concentration of 5 ng/µl.

Generation of pIns-DNNRF-1ER ^{TAM} transgenic mice

pIns-DNNRF-1ER^{TAM} DNA was injected into male pronuclei of day 1-fertilized (CBA × C57BL/6) F1 embryos. Injected embryos were transferred into day 1-plugged pseudopregnant foster mice, and the litters were screened for presence of the transgene by PCR. Founder mice were backcrossed to C57BL/6 for $\geq$ 5 generations to establish transgenic lines. For Southern blot analysis, genomic DNA isolated from mouse tails was digested overnight with BamHI or EcoR1, fractionated on a 1% agarose gel, transferred to a Hybond-N+ filter (Amersham), and probed with a ^{32}P-labeled 0.5 kb human NRF-1 cDNA fragment. Transgene copy number was estimated by densitometry with dilutions of a NotI/HindIII transgene fragment. All subsequent genotyping was done by PCR using the following primer sequences that span DNNRF-1 and the ER^{TAM} (forward 5'ATCAGCAAACGCAAACAC3' and reverse 5'GCCAGACGAGACCAATCAT
C3'). Littermates, or age-matched C57BL/6 mic were used as controls in all experiments.

Generation of pIns-DNNRF-1ER ^{TAM}/ pIns-MycER ^{TAM} double transgenic mice

pIns-MycER ^{TAM} mice (kindly provided by Gerard Evan, UCSF) were crossed with pIns-DNNRF-1ER ^{TAM} mice and screened for the presence of both transgenes using a primer set

consisting of a common 3' primer for the ER region (5'TAGATCATGGGCGGTTCAGC3') and specific 5' primers for DNNRF-1 (as above) and Myc (5'CAAGAGGGTCAAGTT
GGACA3'). These primer sets amplified PCR products of 682 bp and 422 bp, respectively.

Histological, immunohistochemical and histochemical analysis of pancreatic tissue.

Pancreata were excised from mice, and 5 mm pieces of tissue were fixed overnight in 10% neutral-buffered formalin, embedded in paraffin wax, and sectioned (5–10 µm). Immunohistochemical staining and morphometric analysis were performed in tissue sections separated by 200 µM to include > 20 islets. Apoptotic cells were identified in paraffin-embedded sections by immuno-staining with activated cleaved caspase 3 antibody (Cell Signaling Technologies, Inc., Danvers, MA). Immunohistochemistry was performed using guinea pig anti-insulin primary antibody (Fitzgerald Labs, Concord, MA, USA) diluted 1:450, rabbit anti-glucagon primary antibody (Vector Labs, Burlingame, CA) diluted 1:30, visinin-like protein 1 primary antibody (Thermo Scientific Pierce Products) diluted 1:100. Immunostaining was completed using a three-step streptavidin technique, as described (Carson and Hadik, 2004). Histochemistry for cytochrome oxidase and succinate dehydrogenase activities were performed on formalin-fixed and cryosections, respectively, using methods previously described (Morrish et al., 2003; Sweet et al., 2004).

Perifusion system for islets

Islets were harvested and a flow chamber was used to evaluate dynamic oxygen consumption and insulin release by islets in response to glucose, as previously described (Niswender et al., 2005).

Static measurement of insulin secretion

Static insulin secretion was determined with different secretagogues as previously described (Patti et al., 2003). Briefly, islets were transferred into a Petri dish containing Krebs Ringer buffer (KRB), 0.1% BSA and 3 mM glucose and incubated at 37°C in 5% CO_2 for 60 min.

Subsequently, islets were placed into 96-well plates (10 islets/well) containing no glucose, 20 mM glucose, 30 mM KCl, or 20 mM glucose and 30 mM KCl, and incubated for 60 min. At the end of this period, supernatant was assayed for insulin using an RIA kit (Linco Research Inc.). For solutions containing 30 mM KCl, the NaCl concentration in the KRB was reduced by 25 mM.

Electron microscopy

Islets were isolated and fixed for electron microscopy as previously described (Morrish et al., 2003). Cell and mitochondrial areas were calculated using the NIH image processing program ImageJ.

Image J measurements

Images were imported into Image J and the area of each islet was measured using the freehand selection tool. The area in Image J is provided as square pixels with an aspect ratio of 1. For analysis of the cell density in an islet, nuclei were counted and divided by the total area of an islet and the data expressed as nuclei per square pixel. Caspase and insulin immunostaining was quantitated as a percentage of islet area. Mitochondria and insulin secretory granules were quantitated per unit cellular area.

Animals

This study was carried out in strict compliance with the recommendations in the Guide for the Care and Use of Laboratory Animals of the National Institutes of Health. All mouse protocols used in this study were approved by the FHCRC Institutional Animal Care and Use Committee (File #1238). Mice were housed at the FHCRC and fed a regular chow diet. Male mice were used for all experiments. All surgery was performed under sodium pentobarbital anesthesia and all efforts were made to minimize suffering.

Clinical chemistry assays

Blood or urine glucose levels were measured with a portable glucose measuring device (OneTouch, LifeScan, Milpitas, CA), accurate for glucose values between 10 to 600 mg/dl. Serum insulin levels were measured by ELISA (Mouse Phenotyping Center, University of Washington, WA).

All animals used in these studies were between 2 and 8 mos of age. For fasting blood glucose measurements, mice were fasted for 4 h and then placed in a heated chamber (32°C) for 10 min to induce vasodilation. Blood (0.2 ml) was collected from tail veins.

ATP assays

ATP content in freshly isolated islets was measured by the CellTiter-Glo assay (Promega).

Glucose tolerance test and insulin sensitivity assays

For the glucose tolerance test (GTT), mice were fasted overnight (14 h) and injected intraperitoneally with 10% glucose in PBS at a dose of 2 mg glucose/g body wt. For the insulin sensitivity assay, mice were fasted overnight and injected intraperitoneally with 0.1 units/ml Humulin R insulin (Lilly, Indianapolis, IN) in sterile PBS at a dose of 1.0 mU insulin/g body wt.

Statistical analysis

All assays were performed at least 3 times. Statistical analysis was performed using Student's t test. Two-sided p-values of 0.05 were deemed significant. For dynamic insulin secretion, ANOVA (repeated measures) followed by Tukey's Multiple Comparison test was performed using GraphPad Prism (LaJolla, CA).

REFERENCES

Antinozzi, P.A., Ishihara, H., Newgard, C.B., Wollheim, C.B. (2002). Mitochondrial metabolism sets the maximal limit of fuel-stimulated insulin secretion in a model pancreatic beta cell: a survey of four fuel secretagogues. J. Biol. Chem. 277, 11746-11755.

Au, H.C., and Scheffler, I.E. (1998). Promoter analysis of the human succinate dehydrogenase iron-protein gene--both nuclear respiratory factors NRF-1 and NRF-2 are required. Eur. J. Biochem. *251*, 164-174.

Austin, S.A., Vriesendorp, F.J., Thandroyen, F.T., Hecht, J.T., Jones, O.T., Jones, D.R. (1998). Expanding the phenotype of the 8344 transfer RNAlysine mitochondrial DNA mutation. Neurology *51*, 1447-1450.

Becker R, Laube H, Laube H, Linn T, Pabst W, Damian MS. Impaired glucose effectiveness in chronic progressive external ophthalmoplegia. Metabolism 2002; 51: 796-800.

Bensch, K.G., Mott, J.L., Chang, S.W., Hansen, P.A., Moxley, M.A., Chambers, K.T., de Graaf, W., Zassenhaus, H.P., Corbett, J.A. (2009). Selective mtDNA mutation accumulation results in {beta}-cell apoptosis and diabetes development. Am. J. Physiol. Endocrinol. Metab. 296: E672-E680.

Cam, H., Balciunaite, E., Blais, A., Spektor, A., Scarpulla, R.C., Young, R., Kluger, Y., Dynlacht, B.D. (2004). A common set of gene regulatory networks links metabolism and growth inhibition. Mol. Cell *16*, 399-411.

Campbell, J.E., and Newgard, C.B. (2021). Mechanisms controlling pancreatic islet cell function in insulin secretion. Nat. Rev. Mol. Cell. Biol. *22*, 142-58.

Carson, F.L., and Hadik, C. (1997). Histotechnology: A self-instructional text. ASCP Press.

Cho, Y.M., Shin, H.D., Park, B.L., Kim, J.H., Park, K.S., Kim, S.Y., Lee, H.K. (2005). Association between polymorphisms in the nuclear respiratory factor 1 gene and type 2 diabetes mellitus in the Korean population. Diabetologia *48*, 2033-2038.

Dai, F.F., Zhang, Y., Kang, Y., Wang, Q., Gaisano, H.Y., Braunewell, K.H., Chan, C.B., Wheeler, M.B. (2006). The neuronal Ca2+ sensor protein visinin-like protein-1 is expressed in pancreatic islets and regulates insulin secretion. J. Biol. Chem. *281*, 21942-21953.

Dhar, S.S., Liang, H.L., Wong-Riley, M.T. (2009). Nuclear respiratory factor 1 co-regulates AMPA glutamate receptor subunit 2 and cytochrome c oxidase: tight coupling of glutamatergic transmission and energy metabolism in neurons. J. Neurochem. *108*, 1595-1606.

Dhar SS, Ongwijitwat S, Wong-Riley MT. Nuclear respiratory factor 1 regulates all ten nuclear-encoded subunits of cytochrome c oxidase in neurons. J Biol Chem 2008; 283: 3120-3129.

Fu, J., Zhang, J., Jin, F., Patchefsky, J., Braunewell, K.H., Klein-Szanto, A.J. (2009). Promoter regulation of the visinin-like subfamily of neuronal calcium sensor proteins by nuclear respiratory factor-1. J. Biol. Chem. *284*, 27577-86.

Gaulton, K.J., Willer, C.J., Li, Y., Scott, L.J., Conneely, K.N., Jackson, A.U., Duren, W.L., Chines, P.S., Narisu, N., Bonnycastle, L.L., et al. (2008). Comprehensive association study of type 2 diabetes and related quantitative traits with 222 candidate genes. Diabetes *57*, 3136-3144.

Gleyzer, N., Vercauteren, K., Scarpulla, R.C. (2005). Control of mitochondrial transcription specificity factors (TFB1M and TFB2M) by nuclear respiratory factors (NRF-1 and NRF-2) and PGC-1 family coactivators. Mol. Cell. Biol. *25*, 1354-1366.

Gonen, N. And Assaraf, Y.G. (2010) The obligatory intestinal folate transporter PCFT (SLC46A1) is regulated by nuclear respiratory factor 1. J. Biol. Chem. *285*, 33602-33613.

Handschin, C., and Spiegelman, B.M. (2006). Peroxisome proliferator-activated receptor gamma coactivator 1 coactivators, energy homeostasis, and metabolism. Endocr. Rev. *27*, 728-735.

Hong, E.G., Jung, D.Y., Ko, H.J., Zhang, Z., Ma, Z., Jun, J.Y., Kim, J.H., Sumner, A.D., Vary, T.C., Gardner, T.W., et al. (2007). Nonobese, insulin-deficient Ins2Akita mice develop type 2 diabetes phenotypes including insulin resistance and cardiac remodeling. Am. J. Physiol. Endocrinol. Metab. *293*, E1687-1696.

Huo, L., and Scarpulla, R.C. (2001). Mitochondrial DNA instability and peri-implantation lethality associated with targeted disruption of nuclear respiratory factor 1 in mice. Mol. Cell. Biol. *21*, 644-654.

Jensen, M.V., Joseph, J.W., Ronnebaum, S.M., Burgess, S.C., Sherry, A.D., Newgard, C.B. (2008). Metabolic cycling in control of glucose-stimulated insulin secretion. Am. J. Physiol. Endocrinol. Metab. *295*, E1287-1297.

Kang, D., Kim, S.H., Hamasaki, N. (2007). Mitochondrial transcription factor A (TFAM): roles in maintenance of mtDNA and cellular functions. Mitochondrion *7*,39-44.

Karaa, A., and Goldstein, A. (2015). The spectrum of clinical presentation, diagnosis, and management of mitochondrial forms of diabetes. Pediatric Diabetes *16*, 1-9.

Katagiri, H., Asano, T, Ishihara, H., Inukai, K., Anai, M., Yamanouchi, T., Tsukuda, K., Kikuchi, M., Kitaoka, H., Ohsawa, N., et al. (1994). Mitochondrial diabetes mellitus: prevalence and clinical characterization of diabetes due to mitochondrial tRNA(Leu(UUR)) gene mutation in Japanese patients. Diabetologia *37*,504-510.

Kherrouche, Z., De Launoit, Y., Monte, D. (2004). The NRF-1/alpha-PAL transcription factor regulates human E2F6 promoter activity. Biochem. J. *383*, 529-36.

Kobayashi, T., Nakanishi, K., Nakase, H., Kajio, H., Okubo, M., Murase, T., Kosaka, K. (1997). In situ characterization of islets in diabetes with a mitochondrial DNA mutation at nucleotide position 3243. Diabetes *46*,1567-1571.

Koeck, T., Olsson, A.H., Nitert, M.D., Sharoyko, V.V., Ladenvall, C., Kotova, O., Reiling, E., Ronn, T., Parikh, H., Taneera, J. (2011). A common variant in TFB1M is associated with reduced insulin secretion and increased future risk of type 2 diabetes. Cell Metab. *13*: 80-91.

Ladiges, W.C., Knoblaugh, S.E., Morton, J.F., Korth, M.J., Sopher, B.L., Baskin, C.R., MacAuley, A., Goodman, A.G., LeBoeuf, R.C., Katze, M.G. (2005). Pancreatic beta-cell failure and diabetes in mice with a deletion mutation of the endoplasmic reticulum molecular chaperone gene P58IPK. Diabetes *54,* 1074-1081.

Li, F., Wang, Y., Zeller, K.I., Potter, J.J., Wonsey, D.R., O'Donnell, K.A., Kim, J.W., Yustein, J.T., Lee, L.A., Dang, C.V. (2005). Myc stimulates nuclearly encoded mitochondrial genes and mitochondrial biogenesis. Mol. Cell. Biol. *25*, 6225-6234.

Ling, C., Del Guerra, S., Lupi, R., Ronn, T., Granhall, C., Luthman, H., Masiello, P., Marchetti, P., Groop, L., Del Prato S. (2008). Epigenetic regulation of PPARGC1A in human type 2 diabetic islets and effect on insulin secretion. Diabetologia *51*,615-622.

Liu Y., Niu, N., Zhu, X., Du, T., Wang, X., Chen, D., Wu, X., Gu, H.F., Liu, Y. (2008). Genetic variation and association analyses of the nuclear respiratory factor 1 (NRF1) gene in Chinese patients with type 2 diabetes. Diabetes *57*, 777-782.

Maassen, J.A., 'T Hart, L.M., Van Essen, E., Heine, R.J., Nijpels, G., Jahangir Tafrechi, R.S., Raap, A.K., Janssen, G.M., Lemkes, H.H. (2004). Mitochondrial diabetes: molecular mechanisms and clinical presentation. Diabetes *53,* Suppl 1: S103-109.

Maechler, P., Carobbio, S., Rubi, B.. (2006). In beta-cells mitochondria integrate and generate metabolic signals controlling insulin secretion. Int. J. Biochem. Cell Biol. *38,*696-709.

Maedler, K., Spinas, G.A., Dyntar, D., Moritz, W., Kaiser, N., Donath, M.Y. (2001). Distinct effects of saturated and monounsaturated fatty acids on beta-cell turnover and function. Diabetes *50*, 69-76.

Margineantu, D.H., Emerson, C.B., Diaz, D., Hockenbery, D.M. (2007). Hsp90 inhibition decreases mitochondrial protein turnover. PLoS One *2*, e1066.

Matschinsky, F.M., and Collins, H.W. (1997). Essential biochemical design features of the fuel-sensing system in pancreatic beta-cells. Chem. Biol. *4*, 249-257.

Morrish, F., Giedt, C., Hockenbery, D. (2003). c-MYC apoptotic function is mediated by NRF-1 target genes. Genes Dev. 17, 240-255.

Niswender, C.M., Willis, B.S., Wallen, A., Sweet, I.R., Jetton, T.L., Thompson, B.R., Wu, C., Lange, A.J., McKnight, G.S. (2005). Cre recombinase-dependent expression of a constitutively active mutant allele of the catalytic subunit of protein kinase A. Genesis 43, 109-119.

Noda, M., Yamashita, S., Takahashi, N., Eto, K., Shen, L.M., Izumi, K., Daniel, S., Tsubamoto, Y., Nemoto, T., Iino, M., et al. (2002). Switch to anaerobic glucose metabolism with NADH accumulation in the beta-cell model of mitochondrial diabetes. Characteristics of betaHC9 cells deficient in mitochondrial DNA transcription. J. Biol. Chem. *277,* 41817-41826.

Ohashi, P.S., Oehen, S., Buerki, K., Pircher, H., Ohashi, C.T., Odermatt, B., Malissen, B., Zinkernagel, R.M., Hengartner. H. (1991). Ablation of "tolerance" and induction of diabetes by virus infection in viral antigen transgenic mice. Cell *65*, 305-317.

Pascal, S.M., Guiot, Y., Pelengaris, S., Khan, M., Jonas, J.C. (2008). Effects of c-MYC activation on glucose stimulus-secretion coupling events in mouse pancreatic islets. Am. J. Physiol. Endocrinol. Metab. *295*, E92-102.

Patti, M.E., Butte, A.J., Crunkhorn, S., Cusi, K., Berria, R., Kashyap, S., Miyazaki, Y., Kohane, I., Costello, M., Saccone, R., et al. (2003).Coordinated reduction of genes of oxidative metabolism in humans with insulin resistance and diabetes: Potential role of PGC1 and NRF1. Proc. Natl. Acad. Sci. U.S.A. 100, 8466-8471.

Pelengaris, S., Khan, M., Evan, G.I. (2002). Suppression of Myc-induced apoptosis in beta cells exposes multiple oncogenic properties of Myc and triggers carcinogenic progression. Cell *109*, 321-334.

Perseghin, G., Lattuada, G., Danna, M., Sereni, L.P., Maffi, P., De Cobelli, F., Battezzati, A., Secchi, A., Del Maschio, A., Luzi, L. (2003). Insulin resistance, intramyocellular lipid content, and plasma adiponectin in patients with type 1 diabetes. Am. J. Physiol. Endocrinol. Metab. *285*, E1174-1181.

Piantadosi, C.A., and Suliman, H.B. (2008). Transcriptional Regulation of SDHa flavoprotein by nuclear respiratory factor-1 prevents pseudo-hypoxia in aerobic cardiac cells. J. Biol. Chem. *283*, 10967-10977.

Piccolo, G., Aschei, M., Ricordi, A., Banfi, P., Lo Curto, F., Fratino, P. (1989). Normal insulin receptors in mitochondrial myopathies with ophthalmoplegia. J. Neurol. Sci. *94,* 163-172.

Popay, T.M., Wang, J., Adams C.M., Howard, G.C., Codreanu, S.G., Sherrod, S.D., McLean, J.A., Thomas, L.R., Lorey, S.L., Machida, Y.J., et al. (2021). MYC regulates ribosome biogenesis and mitochondrial gene expression programs through its interaction with host cell factor-1. eLife *10*, e60191.

Rubi, B., del Arco, A., Bartley, C., Satrustegui, J., Maechler, P. The malate-aspartate NADH shuttle member Aralar1 determines glucose metabolic fate, mitochondrial activity, and insulin secretion in beta cells. J Biol Chem 279: 55659-66, 2004.

Salles, J.E., Kasamatsu, T., Dib, S.A., and Moises, R.S. (2007). Beta-cell function in individuals carrying the mitochondrial tRNA leu (UUR) mutation. Pancreas *34*, 133-137.

Scarpulla, R.C. (2008). Nuclear control of respiratory chain expression by nuclear respiratory factors and PGC-1-related coactivator. Ann. N.Y. Acad. Sci. *1147*,321-334.

Silva, J.P., Kohler, M., Graff, C., Oldfors, A., Magnuson, M.A., Berggren, P.O., Larsson, N.G. (2000). Impaired insulin secretion and beta-cell loss in tissue-specific knockout mice with mitochondrial diabetes. Nat. Genet. *26*, 336-340.

Stark, R., and Roden, M. (2007). ESCI Award 2006. Mitochondrial function and endocrine diseases. Eur. J. Clin. Invest. *37*, 236-248.

Sweet, I.R., Cook, D.L., DeJulio, E., Wallen, A.R., Khalil, G., Callis, J., Reems, J. (2004). Regulation of ATP/ADP in pancreatic islets. Diabetes *53*, 401-409.

Tokusumi, Y., Zhou, S., Takada, S. (2004). Nuclear respiratory factor 1 plays an essential role in transcriptional initiation from the hepatitis B virus x gene promoter. J. Virol. *78*, 10856-10864.

Unger, R.H., and Grundy S. (1985). Hyperglycaemia as an inducer as well as a consequence of impaired islet cell function and insulin resistance: implications for the management of diabetes. Diabetologia *28*, 119-121.

Wicksteed, B.I., Brissova, M., Yan, W., Opland, D.M., Plank, J.L., Reinert, R.B., Dickson, L.M., Tamarina, N.A., Philipson, L.H., Shostak, A. (2010). Conditional gene targeting in mouse pancreatic β-Cells: analysis of ectopic Cre transgene expression in the brain. Diabetes 59, 3090-3098.

Wiederkehr, A., and Wollheim, C.B. (2012). Mitochondrial signals drive insulin secretion in the pancreatic b-cell. Mol. Cell. Endocrin. *353*, 128-137.

Wu, Z., Puigserver, P., Andersson, U., Zhang, C., Adelmant, G., Mootha, V., Troy, A., Cinti, S., Lowell, B., Scarpulla, R.C., et al. (1999). Mechanisms controlling mitochondrial biogenesis and respiration through the thermogenic activator PGC-1. Cell *98*, 115-24.

Yau, B., Naghiloo, S., Diaz-Vegas, A., Carr, A.V., Van Gerwen. J., Needham, E.J., Jevon, D., Chen, S.-Y., Hoehn, K.L., Brandon, A.E., et al. (2021). Proteomic pathways to metabolic disease and type 2 diabetes in the pancreatic islet. iScience *24*, 103099.

FIGURE LEGENDS

Figure 1.

(A) pIns-*DNNRF-1ER*^{TAM} transgene cassette. The 4.25 kb transgene cassette containing the Ins-1 promoter, *DNNRF-1ER*^{TAM} fusion gene and β globin polyA sequences.

(B) Southern blot analysis of copy number.

(C) Fasting blood glucose levels for control (non-transgenic) and transgenic pIns-*DNNRF-1ER*^{TAM} (DNNRF-1) mice at 8 wk of age (n=9).

(D) Fasting serum insulin concentrations for control and transgenic pIns-*DNNRF-1ER*^{TAM} (DNNRF-1) mice at 8 wk of age (n=9).

(E) Serum C-peptide concentrations for control and transgenic pIns-*DNNRF-1ER*^{TAM} (DNNRF-1) mice at 8 wk of age (n=9).

(F) Glucose response of mice at 30 min after administration of 1 mU/g insulin i.p, expressed as percent of baseline, at 6 months of age (n=4).

(G) Control and transgenic mice were weighed at 10, 16 and 26 wk (n=5).

(H) Photograph of control and DNNRF-1 mice at 26 wk.

Data are representative of 3 replicate experiments. Error bars are standard deviations. **=$p<0.01$, *=$p<0.05$ for comparison of DNNRF-1 versus control.

Figure 2.

Histology and immunohistochemistry studies of pancreatic tissue.

(A, B) H&E staining of pancreatic tissue of control (A) and pIns-*DNNRF-1ER*^{TAM} mice (B).

(C, D) Activated Caspase 3 immunostaining of pancreatic islets of control (C) and pIns-*DNNRF-1ER*^{TAM} mice (D).

(E, F, G, H) Insulin immunostaining of pancreatic islets for control (E) and pIns-*DNNRF-1ER*^{TAM} mice (F) at 2 and 6 m of age (G, H).

Photomicrographs are representative of data from 4 or more mice from each group. All images were taken at 40 X magnification.

Figure 3.

Cytochrome oxidase, succinate dehydrogenase histochemistry and electron microscopy of pancreatic islets.

(A, B) Cytochrome c oxidase staining of pancreatic islets from control (A) and pIns-*DNNRF-1ER*^{TAM} mice. (C, D) Succinate dehydrogenase staining for control (C) and pIns-*DNNRF-1ER*^{TAM} mice (D). Photomicrographs of COX and SDH staining taken at 40 X magnification and representative of n=5 mice. Islets are outlined by dotted line and exocrine tissue labeled Exo. Bar is equivalent to 2 µm.

(E, F) Electron micrographs of pancreatic β cell from control (E) and pIns-*DNNRF-1ER*^{TAM} mice (F) (representative of 10 β cells). All tissues were obtained at 2 mo of age.

Figure 4.

Glucose-stimulated oxygen consumption and insulin secretion from isolated islets. 100 islets were perfused with 3 mM glucose for 30 min. The glucose in the perifusate was subsequently raised to 20 mM for 30 min, followed by sequential addition of 5 µM nimodipine and KCN.

(A) Oxygen consumption rate (OCR) in isolated islets. The ANOVA p values were as follows; 3 mM glucose (p-value<0.001), 20 mM glucose (p-value<0.001), 20 mM glucose+nimodipine (p-value>0.05).

(B) Insulin secretion rate (ISR) in isolated islets. Addition of the calcium channel blocker nimodipine inhibited Ca^{++}-dependent OCR and KCN completely inhibited OCR in control islets. The ANOVA p values were as follows; 3 mM glucose (p value<0.05), 20 mM glucose (p value<0.001), 20 mM glucose+nimodipine (p value<0.001).

Data are means +/- standard deviation of 3 separate experiments.

Figure 5.

Myc corrects fasting blood glucose and glucose tolerance in pIns-*DNNRF-1ER^{TAM}* mice.

(A) Fasting blood glucose in double transgenic pIns-*DNNRF-1ER^{TAM}* /pIns-*MycER^{TAM}* mice with targeted expression of both MycER and DNNRF-1ER to β cells compared with pIns-DNNRF-1ER^{TAM} mice at 2 mo of age.

(B) Glucose tolerance to intraperitoneal injection of 10% glucose in PBS at a dose of 2 mg glucose/g body wt of pIns-*DNNRF-1ER^{TAM}* /pIns-*MycER^{TAM}* mice compared with pIns-DNNRF-1ER^{TAM} mice at 2 mo of age (n=4). These data are representative of 3 separate experiments. **=p<0.01.

Supplemental Tables

Suppl. Table 1. Results for qRT-PCR analysis. Data are mean and SE values derived from analysis of up to 3 independent wild type or DNNRF-1 mice. Mice were age and sex matched.

Suppl. Table 2. Summary of primers used for qRT-PCR.

Supplemental Figures

Suppl. Figure 1. Onset of increase in non-fasting blood glucose in DNNRF-1 mice. Blood glucose levels measured in control and DNNRF-1 mice at 3, 5 and 8 weeks of age (n=8). Data represent means +/- standard deviations. *=p-value <0.05, **=p-value<0.01.

Suppl. Figure 2. Islet morphology. Quantitative analysis of **(A)** islet area, **(B)** nuclei per unit islet area, **(C)** active caspase-3 immunostaining as percent of islet area and **(D)** insulin immunostaining as percent of islet area in 2 mo (black bar) and 6 mo-old (white bar) mice . Data from 3 mice per group with analysis of 20 islets per pancreas from sections separated by 200 µM. *=p<0.05, **=p<0.01

Suppl. Figure 3. Insulin and glucagon immunohistochemistry. Insulin **(A)** and glucagon **(B)** immunostaining for control mice. Insulin **(C)** and glucagon **(D)** staining for pIns-*DNNRF-1ER*^{TAM} mice (n=3).

Suppl. Figure 4. Insulin and visinin-like 1 protein immunohistochemistry. Insulin (A) and visinin-like 1 (B) immunostaining for control mice. Insulin (C) and visinin-like 1 (D) staining for pIns-DNNRF-1ER^{TAM} mice (n=3).

Suppl. Figure 5. Morphometric analysis of β-cell electron micrographs. **(A)** Cellular area of pIns-*DNNRF-1ER*^{TAM} and wildtype β-cells. **(B)** Mitochondria per cell. **(C)** Mitochondrial area normalized to cell area. **(D)** Insulin secretory granules normalized to cell area. Data represent means +/- standard deviations (n=10) **=p<0.01.

Suppl. Figure 6. Static islet assay for response to glucose and KCl. Each static analysis experiment was performed with four replicates of 10 islets per well, treated with glucose at 0 mM (black bar), 20 mM (white bar), 0 mM plus 30 mM KCl (gray bar) and 20 mM glucose plus 30 mM KCl (cross-hatched bar). The data are means +/- standard deviations of 3 replicate experiments. The table included in this figure provides p-values for t-test comparison and ANOVA data for control (wild-type) versus DNNRF-1 mice.

Suppl. Figure 7. ATP levels in isolated islets. ATP content in freshly isolated islets was measured by the CellTiter-Glo assay. Data are means of 3 replicate experiments. For each experiment, ATP was measured from 3 islets in triplicate (controls) and duplicate (transgenics).

Suppl. Figure 8. Islet morphology in pIns-MycER^{TAM}/pIns-DNNRF-1ER^{TAM} mice. H&E staining of pancreatic islet from non-transgenic control (A) and pIns-*DNNRF-1ER*^{TAM} /pIns-*MycER*^{TAM} transgenic mice (B) at 2 mo of age. Insulin staining of pancreatic islets from control (C) and pIns-*DNNRF-1ER*^{TAM} /pIns-*MycER*^{TAM} (D) mice at 2 mo of age. 40 X magnification (n=3).

A

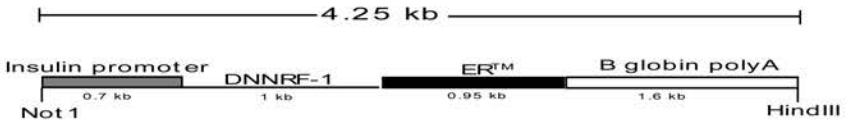
4.25 kb
Insulin promoter
DNNRF-1
ER™
B globin polyA
0.7 kb
1 kb
0.95 kb
1.6 kb
Not 1
HindIII

B

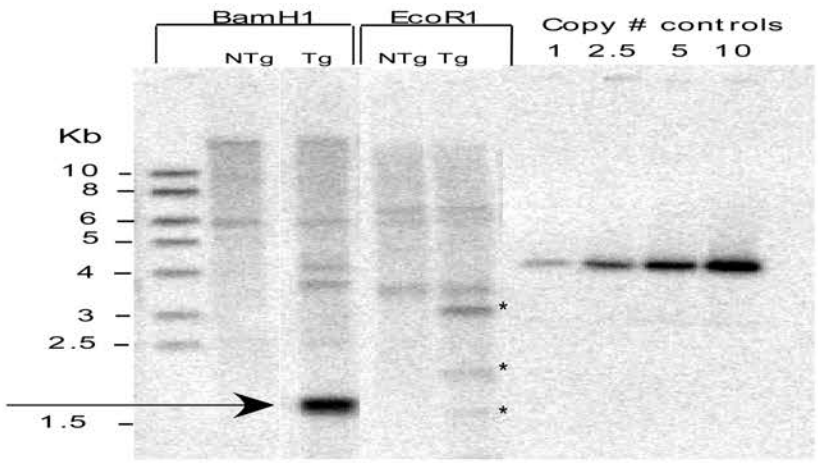
BamH1
EcoR1
Copy # controls
NTg Tg
NTg Tg
1 2.5 5 10
Kb
10
8
6
5
4
3
2.5
1.5

C

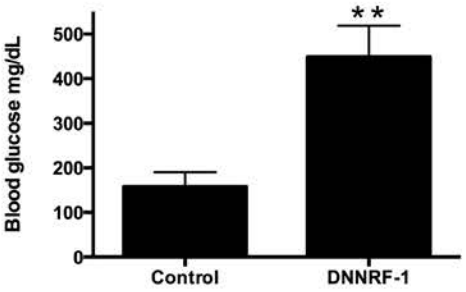
Blood glucose mg/dL
500
400
300
200
100
0
**
Control
DNNRF-1

D

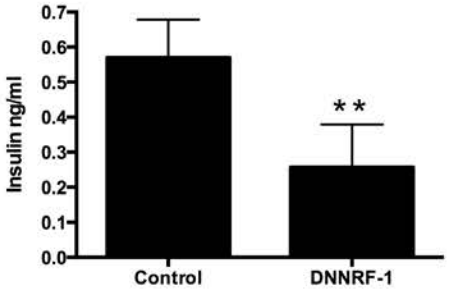
Insulin ng/ml
0.7
0.6
0.5
0.4
0.3
0.2
0.1
0.0
**
Control
DNNRF-1

E

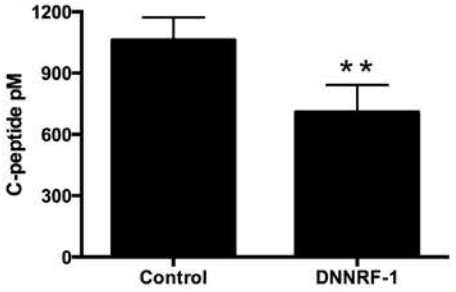
C-peptide pM
1200
900
600
300
0
**
Control
DNNRF-1

F

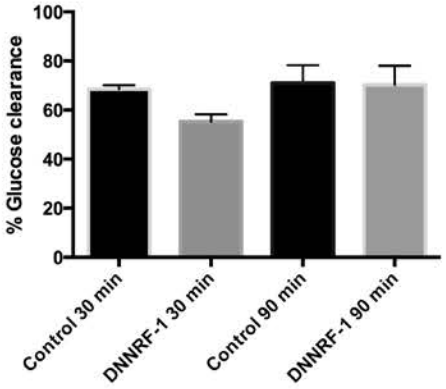
% Glucose clearance
100
80
60
40
20
0
Control 30 min
DNNRF-1 30 min
Control 90 min
DNNRF-1 90 min

G

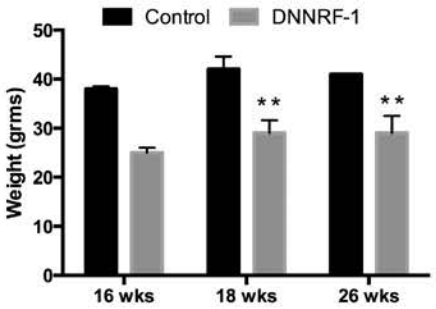
Control
DNNRF-1
Weight (grms)
50
40
30
20
10
0
**
**
16 wks
18 wks
26 wks

H

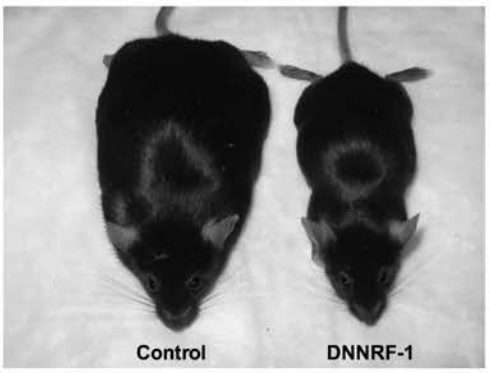
Control
DNNRF-1

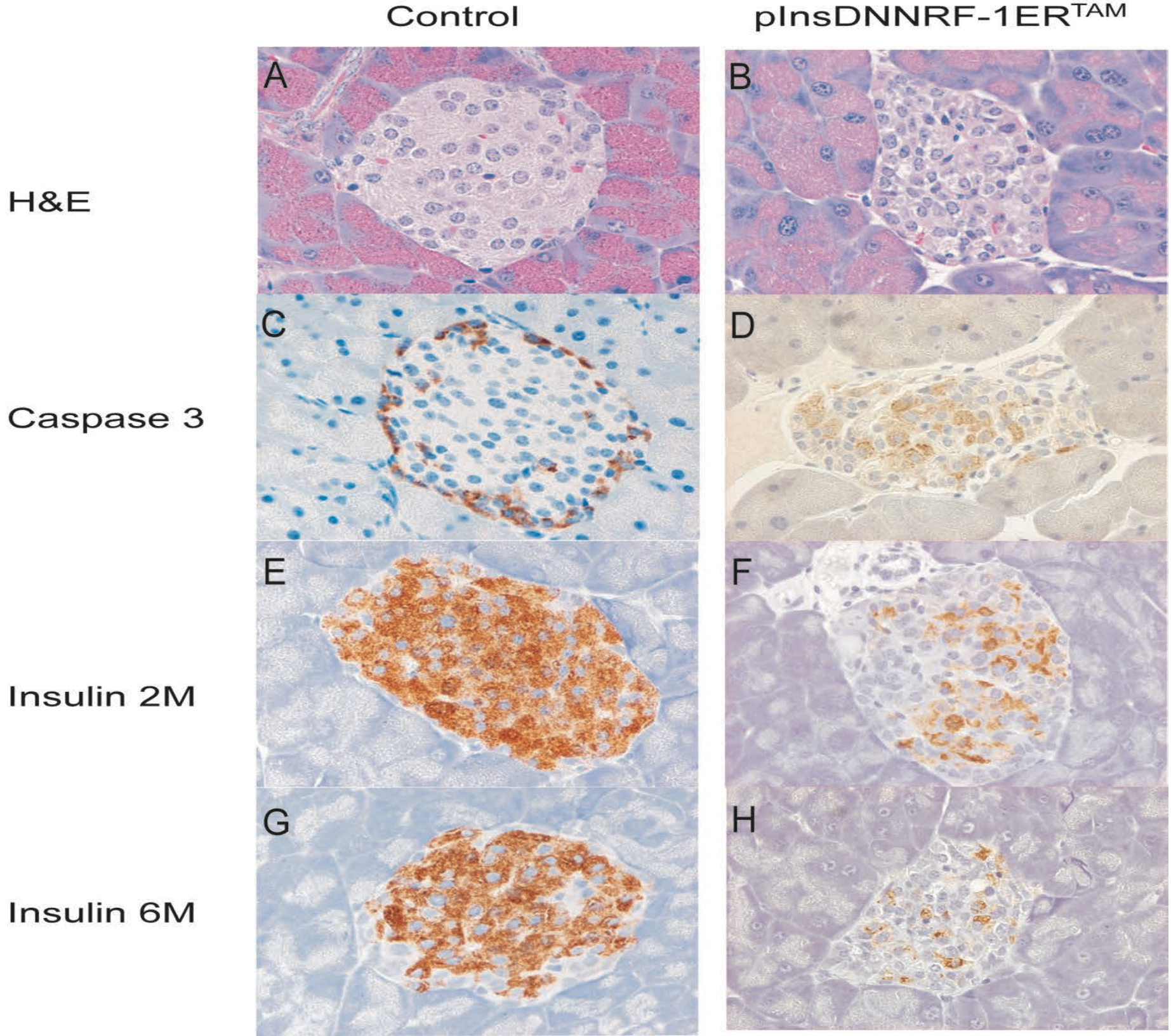
Control
pInsDNNRF-1ERTAM
H&E
Caspase 3
Insulin 2M
Insulin 6M
A
B
C
D
E
F
G
H

Control

pInsDNNRF-1ER^{TAM}

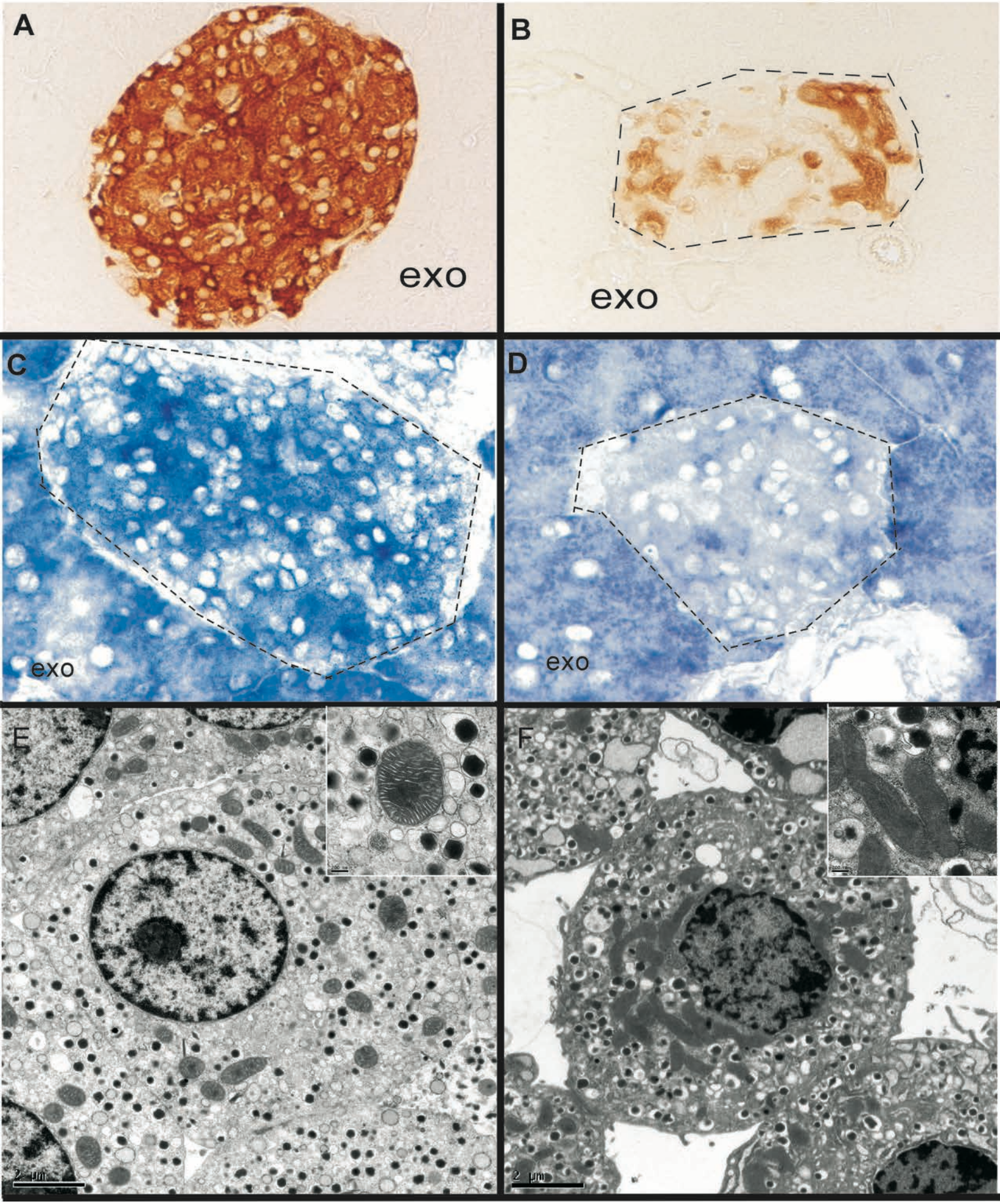

A

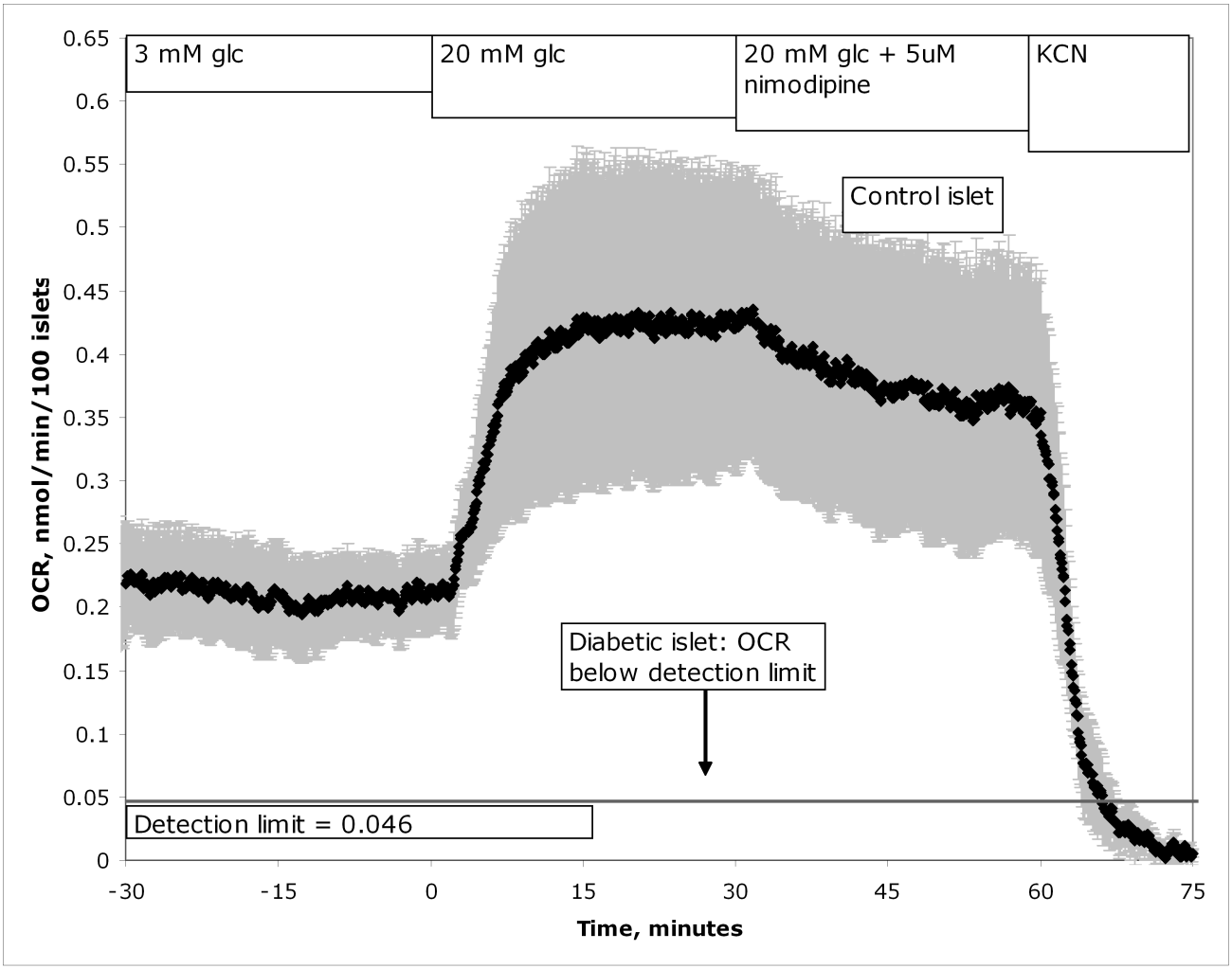
3 mM glc
20 mM glc
20 mM glc + 5uM nimodipine
KCN
Control islet
Diabetic islet: OCR below detection limit
Detection limit = 0.046
OCR, nmol/min/100 islets
Time, minutes
0.65
0.6
0.55
0.5
0.45
0.4
0.35
0.3
0.25
0.2
0.15
0.1
0.05
0
-30
-15
0
15
30
45
60
75

B

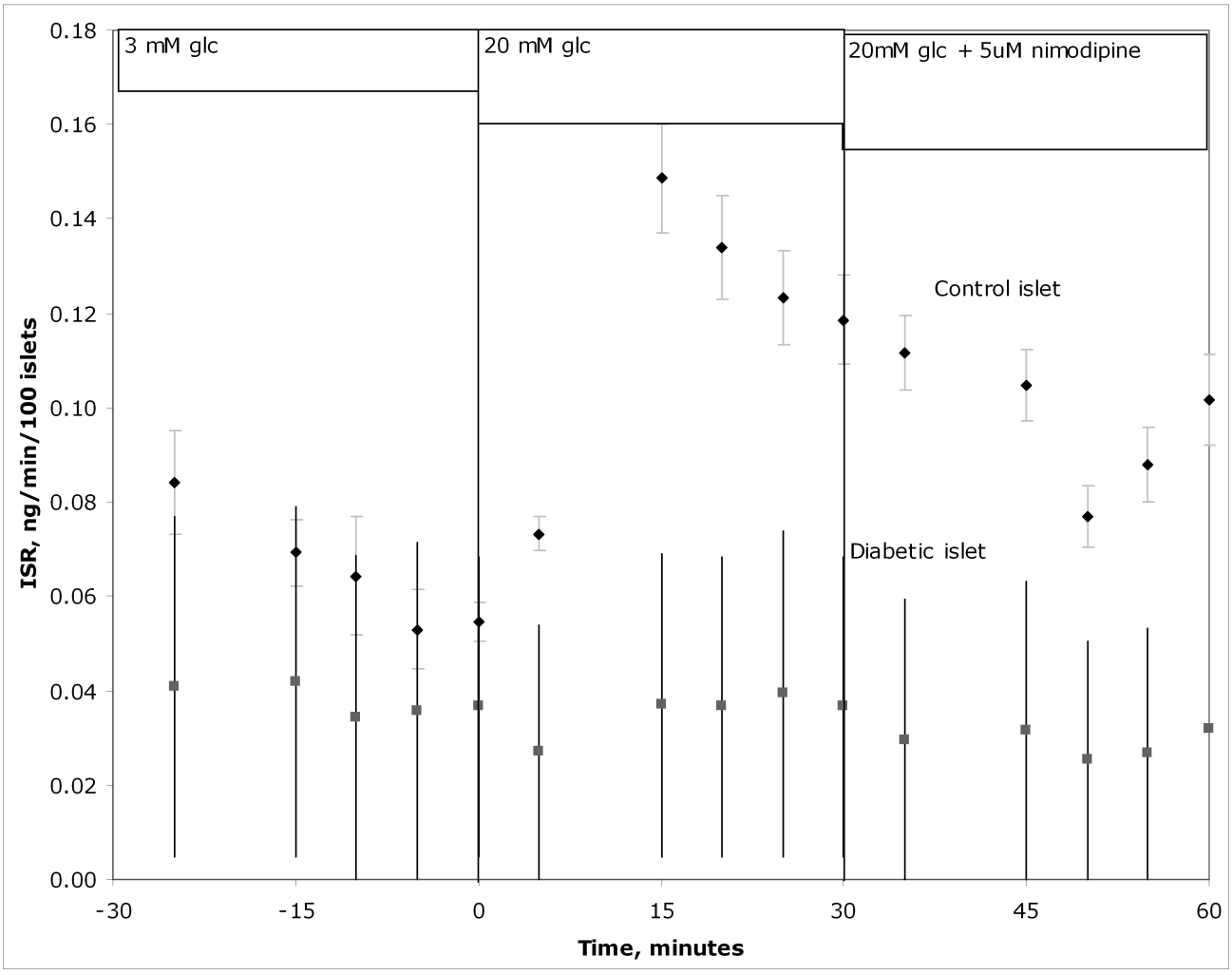
3 mM glc
20 mM glc
20mM glc + 5uM nimodipine
Control islet
Diabetic islet
ISR, ng/min/100 islets
Time, minutes
0.18
0.16
0.14
0.12
0.10
0.08
0.06
0.04
0.02
0.00
-30
-15
0
15
30
45
60

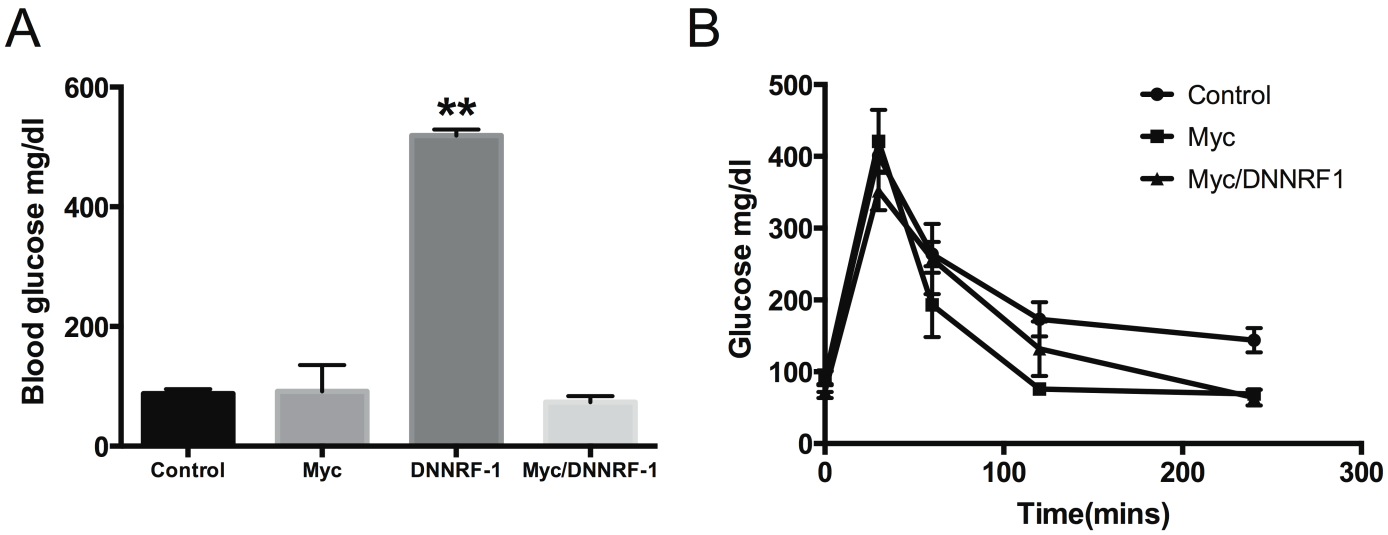
A
Blood glucose mg/dl
600
400
200
0
**
Control
Myc
DNNRF-1
Myc/DNNRF-1
B
Glucose mg/dl
500
400
300
200
100
0
0
100
200
300
Time(mins)
Control
Myc
Myc/DNNRF1